Impedance Spectroscopy of the Electro-oxidation of Methanol on Polished Polycrystalline Platinum

Ryan E. Melnick and G. Tayhas R. Palmore*

Division of Engineering, Brown University, Providence, Rhode Island 02912

Received: August 25, 2000; In Final Form: November 8, 2000

The electro-oxidation of methanol on smooth polycrystalline platinum in the presence of a sulfuric acid solution was investigated using impedance spectroscopy. The impedance response of both the electro-oxidation of methanol and the adsorption of hydrogen were measured directly at potentials where these processes are active. The time dependence of the impedance of the adsorption of hydrogen in the presence of methanol was used as an in situ probe of the formation of methanol adsorption products. Monitoring the formation of methanol adsorption products by this method yielded kinetic information for the electro-oxidation of methanol at low potentials that previously has been difficult to obtain. The fitting of the impedance of the electro-oxidation of methanol to an appropriate model provided the values of impedance parameters whose potential dependence reveal information about the kinetics of the reaction, changes in the coverage of the adsorbed intermediate, and the effect of coadsorbed oxygen containing species. The results indicate the presence of five different potential regions between 40 and 800 mV vs RHE where a change in the reaction mechanism occurs. The mechanistic changes are interpreted as being due to the presence of oxygen containing species with different reactivities at different potentials.

1. Introduction

The recent rise of interest in the electro-oxidation of methanol is driven by the dawning recognition that a practical direct methanol fuel cell (DMFC) is the most promising approach to fuel cell technology with transportation applications. Yet despite the large number of studies conducted using electrochemical or spectroscopic techniques, much remains unknown about the mechanism of this reaction.[1,2] We show that impedance spectroscopy provides new insight into the mechanism of the electro-oxidation of methanol at smooth polycrystalline platinum in sulfuric acid. In addition to providing new mechanistic insights, this study is intended to serve as a guide for future applications of impedance spectroscopy to DMFC research.[3]

At least one reaction pathway in the electro-oxidation of methanol proceeds through an adsorbed intermediate that poisons the surface of the electrode. There is a growing consensus that the adsorbed intermediate is carbon monoxide.[1,2] The oxidative removal of the electrode poison requires a source of oxygen. Early studies identified adsorbed OH formed from the discharge of water on platinum as the source of oxygen,[4,5] and this conclusion continues to be debated in recent reports.[6−12] While current from the electro-oxidation of methanol on polycrystalline platinum can be measured as low as 450 mV,[12] measurable current due to the discharge of water does not occur below 700 mV in cyclic voltammograms of smooth polycrystalline platinum in sulfuric acid. This discrepancy has led to a proposal that the source of oxygen for the electro-oxidation of methanol below 700 mV is adsorbed water.[13−16] The presence of two sources of oxygen, adsorbed water and adsorbed OH, leads to two states for the electro-oxidation of methanol.

The presence of three states in the electro-oxidation of methanol was demonstrated recently.[16] One state was proposed to be the reaction of methanol with adsorbed water, one with adsorbed OH, and the third state at higher potentials included the evolution of oxygen. Using impedance spectroscopy, we demonstrate the existence of *five* states for the electro-oxidation of methanol, not including the state that evolves oxygen. These five states comprise one state that does not have a source of oxygen and four other states representing four different sources of oxygen. Burke et al. propose the presence of incipient hydrous oxides on the platinum surface at several potentials.[17−22] They propose that oxidation of organic compounds can occur with these species as well as adsorbed hydroxy, yielding a total of four chemically distinct sources of reactive oxygen on platinum. Moreover, they report potentials for the formation of these four oxygen species that are strikingly similar to the potentials that we observe using impedance spectroscopy.

2. Experimental Section

2.1. Electrode Preparation and Chemicals. The working electrode, purchased from CH Instruments, Inc., was a 2 mm diameter smooth polycrystalline platinum electrode encased in Kel-F. The electrode was polished through a series of polishing powders beginning with 1.0 μm α alumina, followed with 0.3 μm α alumina, and finished with 0.05 μm γ alumina. Between each polishing, the electrode was rinsed thoroughly with high purity water obtained from a Milli-Q Synthesis filtration system (Millipore) and ultrasonically cleaned for 5 min in Milli-Q water. The polishing procedure produced a mirror-bright surface that under magnification was free from defects or features other than those produced from the 0.05 μm polish. Over the course of the experiments, the electrode occasionally was re-polished to refresh the surface.

Solutions were prepared with Milli-Q water, optima grade sulfuric acid (Fischer), and ACS certified methanol (Fischer). The electrochemical cell was purged using 99.9997% Argon

* To whom correspondence should be addressed: Tayhas_Palmore@brown.edu.

10.1021/jp0030847 CCC: $20.00
Published on Web 01/12/2001

(Air Products) dispensed through a high purity brass regulator (Praxair). The reference electrode was supplied with 99.4% hydrogen (Praxair). Glassware was cleaned in ACS certified plus nitric acid (Fischer).

2.2. Electrochemical Cell and Instrumentation. The electrochemical cell was derived from a micro cell kit from EG&G Princeton Applied Research consisting of a Pyrex bottom and Teflon top containing fittings for electrodes and gas inlets and outlets. A three-electrode configuration was used for all measurements. The counter electrode was a platinum wire sealed in glass, which shared the cell with the working electrode, gas purging capillary, and capillary to the reference electrode. The reference electrode was housed in a separate compartment connected to the cell via a closed glass stopcock and a capillary. The reference electrode comprises a platinized platinum flag immersed in the same solution as the cell with hydrogen bubbled through it. The reference electrode hereafter will be referred to as RHE and all reported potentials are in reference to this electrode. All glassware was cleaned in boiling 50% nitric acid for several hours followed by thorough rinsing with Milli-Q water and drying in an oven. All measurements were made at ambient temperature.

Impedance spectroscopy (IS) was conducted using a Solartron 1255 frequency response analyzer (FRA) interfaced to an EG&G Princeton Applied Research 273A potentiostat through the 273A/92 electrochemical impedance interface. Both instruments were controlled and data acquired through an IEEE−488 General Purpose Interface Bus interfaced to a Gateway 486 PC. IS experiments were controlled with the M398 Electrochemical Impedance Software v. 1.23 (EG&G Princeton Applied Research). Cyclic voltammetry (CV) experiments were run using the M270/250 Research Electrochemistry Software v. 4.23 (EG&G Princeton Applied Research).

2.3. Procedure. For measurements made at each potential, a 0.5 M H_2SO_4 solution was made directly in a clean cell. The electrodes were rinsed with Milli-Q water and the cell assembled. The cell was purged with argon for 10 min by bubbling argon through the solution. The cell was then blanketed with argon for the remainder of the experiment. The surface of the working electrode was cleaned electrochemically by cycling the potential between 0.04 and 1.35 V vs RHE at 50 mV/s until the CV stopped changing. After stepping the potential of the working electrode to the desired value and allowing 30 s for equilibration, the IS of the electrolyte was measured to obtain a background spectrum in the absence of methanol. Measurements were made using the FRA at frequencies from 100 kHz to 1 Hz with samples spaced logarithmically 10 per decade. Immediately following these measurements, the impedance from 1 Hz to 8.85 mHz containing 20 data points spaced logarithmically was obtained using the multisine option of the M398 software. This option applies a multisine curve via the potentiostat and uses Fourier transformation to extract the impedance. The amplitude of the applied potential perturbation was 5 mV rms for all frequencies measured.

Following measurements of the background impedance, the surface of the working electrode was refreshed by cycling the potential from 0.04 to 1.35 V vs RHE at 50 mV/s until the CV stopped changing. The working electrode subsequently was held at 30 mV vs RHE while enough methanol was injected into the cell to yield a 0.5 M solution. Argon was bubbled through the solution for 3 min to allow mixture and thermal equilibration. The electrode was stepped to the potential of interest and measurements identical to those performed for the background impedance spectrum were performed on solutions that contained methanol.

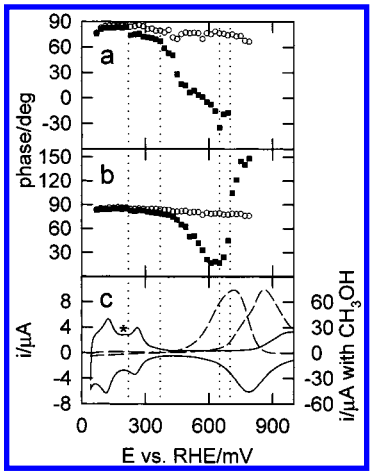

Figure 1. Comparison of the ac phase measured at (a) 0.06 Hz and (b) 1 Hz with (c) the cyclic voltammetry of smooth polycrystalline platinum in 0.5 M H_2SO_4 with (squares and dashed line) and without (circles and solid line) 0.5 M CH_3OH. The cyclic voltammetry sweep rate was 50 mV/s. The vertical dotted lines indicate the potentials (220, 370, 650, 700 mV) where there is a significant change in the phase when methanol is present.

2.4. Data Fitting. IS data were fit to the appropriate models using a modified version of the fitting software LEVM v. 7.1.[23] All other fitting procedures described in this paper were conducted using Table Curve 2D v. 4 (SSPS Inc.).

3. Results

3.1. Qualitative Results. *3.1.1. Phase vs Potential.* Results from IS measurements can be depicted in a number of formats depending on the variables of interest. Applicable variables in this study include real and imaginary components of impedance, impedance phase and magnitude, frequency of the applied ac signal, electrode potential, and time after stepping the electrode to the potential of interest. The phase measured at two frequencies as a function of electrode potential is shown in Figure 1 and compared to results from cyclic voltammetry. The phase at each potential was obtained from the first multisine impedance scan taken after the electrode potential was stepped to the value of interest. The time delay between the potential step and the start of the multisine impedance scan ranged from 691 to 727 s. The vertical dotted lines in Figure 1 correspond to the potentials where the phase indicates a significant change in the impedance. At potentials lower than 230 mV, the phase of the impedance is nearly identical in the presence or absence of methanol. At 230 mV, however, there is an abrupt decrease in the phase of the impedance when methanol is present. This change is best observed at 0.06 Hz (Figure 1a). As seen in the cyclic voltammogram of 0.5 M H_2SO_4 at polycrystalline platinum in the absence of methanol (Figure 1c), this potential (i.e., 230 mV) corresponds to the region where strongly adsorbed hydrogen begins to desorb. This potential is slightly positive of the small anodic peak (indicated with an asterisk in Figure 1c) often observed between the two peaks that correspond to weakly and strongly adsorbed hydrogen in the cyclic voltammogram of 0.5 M H_2SO_4 at polycrystalline platinum. Earlier studies demonstrated that an anodic peak due to the electrooxidation of methanol is observed in the potential region of strongly adsorbed hydrogen on platinum electrodes during the first potential sweep of solutions containing $HClO_4$ as the

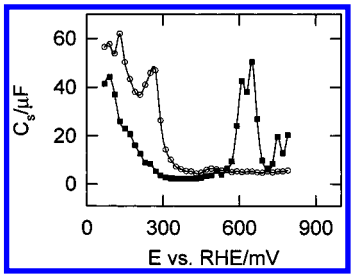

Figure 2. Series capacitance at 1 Hz obtained from the impedance of smooth polycrystalline platinum in 0.5 M H_2SO_4 with (squares) and without (circles) 0.5 M CH_3OH. The lines are provided as a guide and do not represent a fit to the data.

electrolyte and on Pt−Ru alloy electrodes.[7,8,12,24] More recently it has been shown that anodic current greater than that due to the oxidation of adsorbed hydrogen is observed during the first potential sweep of platinum electrodes in solutions of methanol and sulfuric acid at potentials greater than 120 mV.[25] Thus, the abrupt change in the phase at 230 mV in Figure 1a mirrors earlier observations that current in the region of strongly adsorbed hydrogen is due to the electro-oxidation of methanol at an un-poisoned electrode.

In the presence of methanol, the observed phase (measured either at 0.06 or 1 Hz) continues to decrease in value with increasing potential up to 650 mV, at which point the phase at 1 Hz begins to increase (Figure 1b). At 370 mV, the phase at 0.06 Hz begins to decrease more rapidly with increasing potential. At about 500 mV, the phase measured at 0.06 Hz becomes negative (Figure 1a). Negative phase angles are indicative of inductive behavior. Inductive behavior often is observed in systems containing adsorbed intermediates and was observed recently at the anode of a DMFC.[3]

At 700 mV, the phase at 1 Hz increases above 90° (Figure 1b). Phase angles larger than 90° indicate the presence of a negative charge transfer resistance that usually results from passivation of the electrode surface. Passivation of the electrode is probably due to the reversible formation of oxide species often thought to be chemisorbed hydroxy radicals. Anodic current due to oxide formation commences at 700 mV and is observed in the cyclic voltammogram in the absence of methanol (Figure 1c). This current is low until the potential reaches 800 mV. The rapid increase in current at 700 mV in the cyclic voltammogram with methanol present (Figure 1c), however, indicates that the chemisorbed hydroxy radicals significantly increase the rate at which methanol is electro-oxidized.

3.1.2. Series Capacitance vs Potential. Series capacitance is another qualitative representation of impedance as a function of potential (Figure 2). Series capacitance is given by

$$C_s = \frac{-1}{Z''\omega} \qquad (1)$$

where Z'' is the imaginary component of impedance and ω is angular frequency. When methanol is absent, the series capacitance of platinum in sulfuric acid follows the shape of the peaks in the cyclic voltammogram that correspond to adsorbed hydrogen (Figure 1c).[26,27] Neglecting effects from frequency dispersion, the series capacitance for adsorption of hydrogen at low frequencies is the sum of the double-layer capacitance and the pseudo-capacitance of hydrogen adsorption.[28] When methanol is present, methanol adsorption products block sites for the adsorption of hydrogen, thereby reducing the series capacitance. Fewer sites for the adsorption of hydrogen cause a decrease in the corresponding pseudo-capacitance. The decrease in series

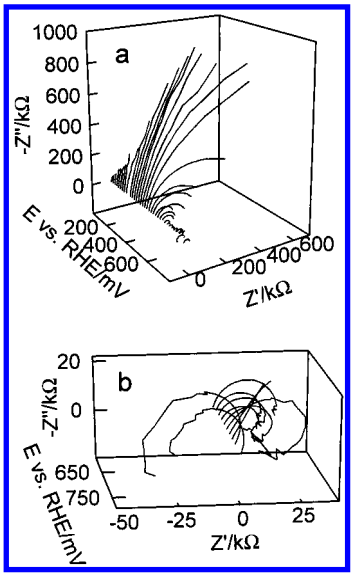

Figure 3. Complex plane plots of the impedance of smooth polycrystalline platinum in 0.5 M H_2SO_4 and 0.5 M CH_3OH from (a) 70 to 790 mV and from (b) 590 to 790 mV. The frequency range is from 8.85 mHz to 100 kHz.

capacitance is more severe in the region of potential that corresponds to strongly adsorbed hydrogen (i.e., 200−350 mV), indicating a high coverage of methanol adsorption products at these potentials. The series capacitance in the absence of methanol is constant at higher potentials. In the presence of methanol, the series capacitance measured at 1 Hz begins to increase at about 430 mV, reaching a maximum at 650 mV, decreasing to the background capacitance at 710 mV, and then again increasing. The series capacitance peak at 650 mV (Figure 2) corresponds to the minimum in the phase at 1 Hz (Figure 1b). The potential of this peak also corresponds to the potential at which there is a maximum in adsorbed CO observed in some IR measurements.[10,11,24]

3.1.3. Complex Plane Representation. The most common way to depict an entire impedance spectrum is in the complex plane. Shown in Figure 3 are complex plane plots of impedance spectra taken from the first impedance scan as a function of electrode potential. The axes labeled Z' and Z'' represent real and imaginary components of impedance, respectively. The value of frequency in each impedance spectrum increases toward the origin. Features of the impedance spectra at high frequencies are not apparent in Figure 3 due to the scale of the axes. These features stem from the rapid adsorption and desorption of hydrogen and will be discussed later. The complex-plane plot of impedance at potentials <230 mV is linear at low frequencies both in the presence or absence of methanol. When methanol is present, the region of low frequency in the impedance spectrum reveals the onset of a semicircle at potentials ≥ 230 mV. This onset corresponds to the sudden change in the phase observed at 230 mV in Figure 1a. From 370 to 650 mV, the diameter of the primary semicircle decreases with increasing potential, indicating a process activated by potential. An impedance semicircle that decreases with increasing potential was observed previously during the electro-oxidation of methanol on carbon supported Pt−Sn electrodes[29] and Pt−Ru electrodes.[3,30] From 650 mV to higher potentials, the diameter of the primary semicircle begins to increase with increasing potential until at 710 mV, the semicircle flips over to the second quadrant of the complex plane. Figure 3b provides a magnified view of the semicircle with increasing diameter and subsequent flipping to the second quadrant. The increase in the diameter

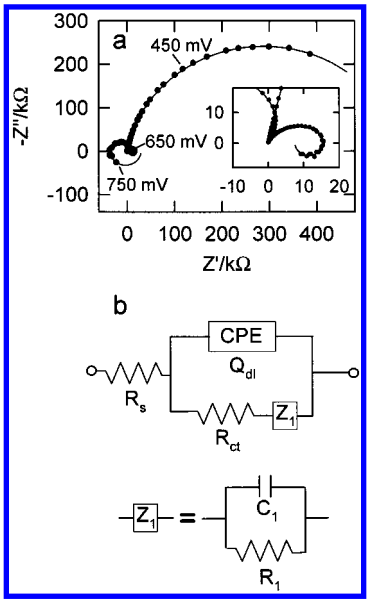

Figure 4. (a) Complex plane plots of the impedance of smooth polycrystalline platinum in 0.5 M H_2SO_4 and 0.5 M CH_3OH at 450, 650, and 750 mV. The frequency range is from 61.95 mHz to 501.19 Hz. The inset provides greater detail of the 650 mV spectrum. The lines represent the fit of the data to (b) the equivalent circuit for the electro-oxidation of methanol. Z_1 was not included for the fit of the circuit to the 450 mV spectrum but was included for the fit of the circuit to the 650 and 750 mV spectra.

of the semicircle corresponds to increasing phase in Figure 1b. The flipping over to the second quadrant corresponds to the phase measured at 0.06 Hz becoming larger than 90°. At about 500 mV, impedance data plotted in the complex plane extends into the fourth quadrant, indicating inductive behavior. This result mirrors the inductive behavior observed for the phase measured at 1 Hz (Figure 1a). At higher potentials, the inductive part of the impedance spectrum develops into a second semicircle in the fourth quadrant of the complex plane (Figure 3b). After the flipping of the primary semicircle into the second quadrant of the complex plane, this second semicircle is apparent in the third and fourth quadrants. The transition from capacitive behavior (i.e., impedance data points measured in the first quadrant only) to inductive behavior at low frequencies is gradual and grows in from the lowest frequencies measured (Figure 1a). Consequently, we believe that a second semicircle is present at all potentials including the 230−500 mV range. To observe the second semicircle, however, requires frequencies lower than those available with our instrumentation.

These two semicircles may be ascribed solely to reaction processes since diffusion effects are not observed or expected for the concentration of methanol used. Several derivations for the impedance of such reactions exist in the literature,[31−35] which indicate that two semicircles in a complex-plane plot of impedance signifies a reaction with one adsorbed intermediate. Considering the complexity of the reaction to electro-oxidize methanol completely, more than one adsorbed intermediate is likely to be present in the reaction pathway.[2,5] Our impedance results, however, indicate that the rate of turnover of all but one intermediate is very fast.

3.2. Quantitative Results. The derivation for the impedance of a reaction with one adsorbed intermediate is given in the appendix (eq A-8) and it predicts the equivalent circuit given in Figure 4b with the impedance element Z_1 included. Fitting the equivalent circuit to the data provides the values of the circuit parameters, which can be related to the physical quantities inherent in the reaction. When impedance plotted in the complex plane does not reveal the effects of a second semicircle due to experimental constraints on the frequency range, a simplified equivalent circuit (i.e., Z_1 absent) is used instead. Figure 4a shows the complex plane plot of impedance of the electro-oxidation of methanol measured at 450, 650, and 750 mV. The impedance spectrum at 450 mV is typical for the electro-oxidation of methanol between 230 and 470 mV. The solid line is the fit of the data to the equivalent circuit of Figure 4b with the impedance element Z_1 excluded.

At potentials 470 mV and higher, the effects of a second semicircle are observed in the complex plane plots of the impedance for the electro-oxidation of methanol. The impedance spectrum at 650 mV plotted in Figure 4a is typical for the electro-oxidation of methanol between 470 and 700 mV. The solid line is the fit of the data to the equivalent circuit given in Figure 4b, which includes the impedance element Z_1.

Above 700 mV, the primary semicircle in the complex plane flips to the second quadrant with the real component of the impedance becoming negative. The impedance spectrum at 750 mV plotted in Figure 4a is typical for the electro-oxidation of methanol at these potentials. The data still can be fit to the equivalent circuit of Figure 4b with some of the circuit elements having different signs than the fits below 700 mV.

To obtain a satisfactory fit of the data to the circuit in Figure 4b, it was necessary to replace the double layer capacitor with a constant phase element (CPE). The impedance of a CPE is given by

$$Z_Q = \frac{1}{Qs^{\alpha}} \tag{2}$$

where $s \equiv j\omega$ and $j \equiv \sqrt{-1}$. If $\alpha = 1$, the impedance of a CPE is identical to the impedance of a capacitor and Q becomes the capacitance. It has been observed that in the absence of faradaic processes, the double-layer impedance of solid electrodes often exhibit CPE behavior instead of pure capacitive behavior. It also has been observed that in the presence of faradaic processes, the impedance of solid electrodes is distorted, often in such a way that any semicircles present in the complex plane are depressed. The most widely accepted explanation for the presence of CPE behavior and depressed semicircles on solid electrodes is microscopic roughness, causing a coupling of the solution resistance and the double-layer capacitance. Systems such as these can be described in terms of fractal geometry and it has been demonstrated using the fractal formalism that CPE behavior in the absence of faradaic processes is predicted.[36] This formalism also has been extended to cases containing faradaic processes.[37]

We have attempted to analyze the impedance data for the electro-oxidation of methanol and adsorption of hydrogen (described later) using the models obtained assuming fractal geometry in the presence of these faradaic processes. In all cases, these attempts have proved unsuccessful, indicating that microscopic roughness cannot be the sole cause of the nonideal behavior observed in the impedance spectra. This result is consistent with the proposal that CPE behavior observed on electrodes without faradaic processes cannot be due to the geometry of surface roughness because such effects would only be detectable at frequencies on the order of 10 kHz and higher.[38] All data measured for this study exhibited CPE behavior at frequencies much lower than 10 kHz. Experimental evidence also has been provided that demonstrates that a very rough platinum electrode does not exhibit CPE behavior under certain conditions.[38]

A second proposal for the source of observed CPE behavior in the absence of faradaic processes is an inhomogeneous distribution in the value of the double-layer capacitance across the electrode surface.[39] This inhomogeneity would be expected especially in the case of polycrystalline electrodes as the double-layer capacitance depends on the exposed crystal face. The source of the CPE behavior in this case, however, still would be the coupling of the solution resistance and the double-layer capacitance and thus have the same frequency constraints as a rough electrode.[38]

The final possibility for the source of CPE behavior is that it is an intrinsic property of the double-layer.[38,39] This possibility is the only one that allows the replacement of the double-layer capacitor with a CPE in the presence of faradaic processes and is the one that we favor based on the fitting of our experimental data. The source for this intrinsic double-layer behavior has been proposed to be processes involving the adsorption of ions and energetic inhomogeneities on the electrode surface.[38,40]

The expressions for the circuit elements of the equivalent circuit in Figure 4b in terms of physical parameters are given in the appendix (eq A-9). It can be seen that the charge-transfer resistance, R_{ct}, is the only circuit element that has a simple physical meaning. Specifically, the inverse charge-transfer resistance describes how fast the rate of charge transfer for the electro-oxidation of methanol changes with changing electrode potential when the coverage of the intermediate is held constant. It can be thought of as describing the potential dependence of the rate constants for charge transfer. In addition to the charge-transfer resistance, three other physical parameters can be derived from the impedance expression given in eq A-8. At zero frequency, the impedance in eq A-8 reduces to the impedance of a simple resistor. This resistor, known as the faradaic resistance, R_f, is equal to the inverse of the slope of the dc polarization curve and hence is given by

$$R_f^{-1} = \frac{di}{dE} = F\frac{dr_{ct}}{dE} \tag{3}$$

Because the rate of charge transfer, r_{ct}, depends on the intermediate coverage, θ, and the electrode potential, E (see eq A-3), the ordinary derivative of the charge-transfer rate with respect to potential may be expressed as

$$\frac{dr_{ct}}{dE} = \left(\frac{\partial r_{ct}}{\partial E}\right)_\theta + \left(\frac{\partial r_{ct}}{\partial \theta}\right)_E \frac{d\theta}{dE} \tag{4}$$

This expression reveals two contributions to how fast the rate of charge transfer changes with a change in potential (i.e., the slope of the dc polarization curve, R_f^{-1}). The first term indicates how fast the rate of charge transfer changes at constant intermediate coverage (the inverse charge-transfer resistance) and the second term indicates how fast the rate of charge transfer changes with the change in coverage caused by a change in potential. We relate the second term to a parameter we refer to as the coverage resistance, R_c, making the definition

$$R_c \equiv \frac{1}{F\left(\frac{\partial r_{ct}}{\partial \theta}\right)_E \frac{d\theta}{dE}} \tag{5}$$

In terms of the circuit elements in the equivalent circuit in Figure 4b, the zero frequency impedance of the faradaic branch of the circuit is given by

$$Z(\omega=0) = R_{ct} + R_1 = R_f \tag{6}$$

TABLE 1: Physical Parameters Obtained from the Impedance Spectroscopy of the Electro-oxidation of Methanol

	R_f^{-1}	R_{ct}^{-1}	R_c^{-1}	t
physical expression	$\frac{di}{dE}$	$F\left(\frac{\partial r_{ct}}{\partial E}\right)_\theta$	$F\left(\frac{\partial r_{ct}}{\partial \theta}\right)_E \frac{d\theta}{dE}$	$-\frac{N}{N_A}\left(\frac{\partial r_\theta}{\partial \theta}\right)_E^{-1}$
circuit definition	$\frac{1}{R_{ct}+R_1}$	$\frac{1}{R_{ct}}$	$-\frac{R_1}{R_{ct}(R_{ct}+R_1)}$	$\frac{R_{ct}R_1C}{R_{ct}+R_1}$

Experimentally, the zero frequency impedance and thus the faradaic resistance, R_f, is the zero frequency intercept of the real axis in the complex plane. This value can be seen in Figure 4a as the extrapolation of data fitting to zero frequency.

Combining eqs 3−6 and using the definition of the charge-transfer resistance (eq A-9), the following is obtained for the inverse faradaic resistance:

$$R_f^{-1} = \frac{1}{R_{ct}+R_1} = R_{ct}^{-1} + R_c^{-1} \tag{7}$$

This equation can be solved to find the coverage resistance in terms of the circuit elements in the circuit in Figure 4b:

$$R_c = -\frac{R_{ct}(R_{ct}+R_1)}{R_1} \tag{8}$$

The sign of R_c indicates whether the change in coverage induced by a change in electrode potential increases or decreases the rate of charge transfer. At all potentials $\geq$470 mV, where R_c is determined from the data fit to the circuit in Figure 4b, R_c was found to be positive, indicating that the change in coverage with potential increases the rate of charge transfer at these potentials.

It is possible to combine further the circuit parameters in eq A-9 to obtain a parameter we refer to as the coverage relaxation time, τ, which indicates how fast the coverage of the intermediate will relax back to its equilibrium value after perturbation. The coverage relaxation time is given by

$$\tau \equiv \frac{R_{ct}R_1C}{R_{ct}+R_1} = \frac{-1}{\frac{N_A}{N}\left(\frac{\partial r_\theta}{\partial \theta}\right)_E} \tag{9}$$

The sign of τ indicates whether increasing the coverage decreases or increases the rate of the coverage buildup. It is expected that τ would always be positive, indicating that the rate of coverage buildup will decrease as coverage increases and indeed this prediction is supported by our measurements. The sign of the product $R_c\tau$ determines whether the second semicircle observed in the complex plane for systems containing one adsorbed intermediate is inductive or capacitive. A positive value for the product $R_c\tau$ indicates inductive behavior as is observed in our case. Because τ is expected to be positive, the presence of inductive behavior indicates that the change in coverage induced by a change in potential increases the rate of charge transfer while capacitive behavior indicates that the change in coverage decreases the rate of charge transfer.

All four physical parameters obtained from the fit of the IS data for the electro-oxidation of methanol to the equivalent circuit in Figure 4b along with their physical meanings and definitions in terms of the circuit elements in Figure 4b are summarized in Table 1. The four parameters are plotted in Figure 5 as a function of electrode potential. At potentials lower than 470 mV, only R_{ct} can be determined since the impedance

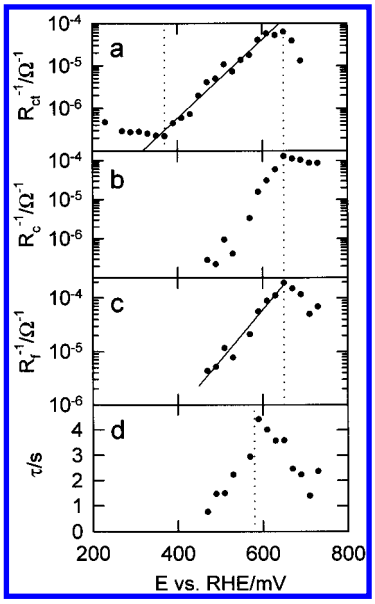

Figure 5. Physically significant parameters plotted as a function of electrode potential. Data were obtained from the fits of the impedance spectra to the equivalent circuit in Figure 4b. (a) Inverse charge-transfer resistance. (b) Inverse coverage resistance. (c) Inverse faradaic resistance. (d) Coverage relaxation time. The solid lines represent fits to the data. The vertical dotted lines illustrate potentials where the impedance parameters indicate a change in the mechanism for the electro-oxidation of methanol at polycrystalline Pt. Negative values of the inverse charge-transfer resistance are not plotted.

element Z_1 must be excluded from the circuit in Figure 4b during data fitting. R_{ct} can be determined starting at 230 mV where the start of the low frequency semicircle is observed in the complex plane. Up to 370 mV, the inverse charge transfer resistance decreases slightly at which point it begins to increase exponentially until a potential of 650 mV is reached (Figure 5a). The exponential increase in the inverse charge-transfer resistance between 370 and 650 mV can be fit to a Tafel line with a slope of 108 mV/decade. At potentials more positive then 650 mV, the inverse charge-transfer resistance begins to decrease with more positive potentials. Above 700 mV, the inverse charge-transfer resistance becomes negative in value, which corresponds to the phase measured at 0.06 Hz becoming larger than 90° (Figure 1b) and the primary semicircle in the complex plane flipping to the second quadrant (Figure 3).

Values for the three other parameters can be determined above 470 mV. Both the inverse coverage resistance and the inverse faradaic resistance increase exponentially with increasing potential up to 650 mV where they both begin to decrease (Figure 5b,c). Unlike the inverse charge transfer resistance, the inverse coverage resistance and the inverse faradaic resistance do not reach negative values in the range of potentials measured. The exponential increase in the inverse faradaic resistance can be fit to a Tafel line with a slope of 106 mV/decade. The value of this slope represents the Tafel slope that would be measured by direct current techniques and can be compared to the previously reported value of 128 mV/decade that was measured between 400 and 500 mV.[15] The decrease in the inverse faradaic resistance starting at 650 mV indicates that non-Tafel behavior is observed at these potentials. This non-Tafel behavior corresponds to the near linear current observed in the cyclic voltammogram starting at this potential (Figure 1c). The final parameter, the coverage relaxation time, increases linearly up to 570 mV where it suddenly begins to decrease linearly (Figure 5d).

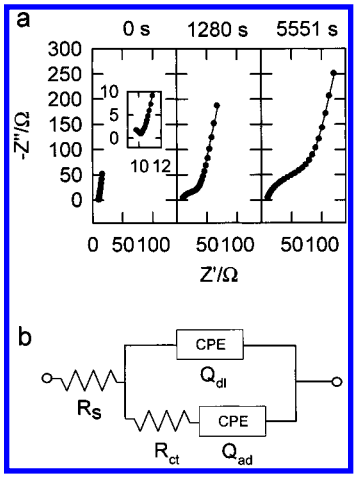

Figure 6. (a) Complex plane plots of the impedance spectra of smooth polycrystalline platinum in 0.5 M H_2SO_4 and 0.5 M CH_3OH as a function of time after injection of methanol. The frequency range was from 100 Hz to 100 kHz. The inset reveals the presence of a semicircle at high frequencies. A full semicircle is not observed due to the limitations of the instrumentation. (b) The equivalent circuit for the hydrogen adsorption reaction, to which the lines in the impedance spectra are fitted.

3.3. Impedance Spectroscopy of upd Hydrogen. In the region of adsorbed hydrogen (upd) on polycrystalline platinum (40−350 mV), the complex plane plot of the impedance spectrum measured in 0.5 M H_2SO_4 consists of a semicircle at high frequencies and a near-vertical line at lower frequencies (Figure 6a, $t = 0$ s). This spectrum is typical for a reaction containing adsorbed reactants and/or products, as is the case for adsorption of hydrogen. The feature due to the adsorption of hydrogen at high frequencies has been observed previously on polycrystalline and single-crystal platinum electrodes.[27,41−44] In the presence of methanol, repetitive scanning of the impedance spectrum reveals the diameter of the semicircle increases with time (Figure 6a, $t = 1280$ s and $t = 5551$ s). This increase reflects the blocking of sites for the adsorption of hydrogen by methanol adsorption products and provides an in situ probe of the blocking process.

Blocking of sites for adsorption of hydrogen can be quantified by fitting the impedance spectra to the appropriate impedance model. Impedance models for this reaction have been derived previously and can be expressed in terms of an equivalent electrical circuit.[26−28,41−45] The impedance for reactions containing adsorbed reactants and/or products can be treated as a special case of the impedance for a reaction with one adsorbed intermediate. Using this approach, the impedance for hydrogen adsorption is given in eq A-11. The equivalent circuit used to fit the data for hydrogen adsorption is given in Figure 6b and the fit is illustrated in Figure 6a (solid lines).

To obtain a satisfactory fit of the data to the circuit depicted in Figure 6b, it was necessary to replace both the double layer capacitor and the adsorption capacitor with a (CPE). No attempt was made to justify theoretically the placement of a CPE in the faradaic branch of the equivalent circuit. Previously, however, such a placement was found to be necessary in the case of hydrogen evolution at platinum and other electrocatalytic surfaces.[46−48] Although not analyzed in terms of a CPE, Glarum and Marshall found a frequency dispersion present in the faradaic impedance due to upd adsorption of hydrogen.[42] Bai et al. found that during hydrogen evolution on platinum, the double-layer CPE acted as a pure capacitor with $\alpha = 1$ while the CPE in the faradaic branch had α values significantly lower than one.[46] We obtained similar results for upd adsorption of

hydrogen in the absence of methanol. Since adsorption of hydrogen is one of the steps in hydrogen evolution, it is not surprising that there are similarities in the frequency dispersion of the adsorption pseudo-capacitance in both hydrogen evolution and upd adsorption of hydrogen. Apparently, something inherent to adsorption of hydrogen gives rise to CPE behavior. Heterogeneity in the adsorption of hydrogen seems apparent from the duel peaks in the cyclic voltammogram (Figure 1c) and series capacitance peaks (Figure 2) and it could be speculated that the CPE behavior is due to this heterogeneity. Glarum and Marshall considered this possibility, however, and concluded that the observed frequency dispersion was not severe enough to warrant this speculation.[42] Nevertheless, it seems probable that the CPE behavior in the faradaic branch is related to the apparent heterogeneity of the hydrogen adsorption process. It is interesting to note in this respect that CPE behavior was not observed during upd adsorption of hydrogen on single-crystal platinum electrodes.[43]

With methanol present, we found that α for the double-layer CPE became lower than one, decreasing as the coverage of methanol adsorption products increases with time. This result may reflect the heterogeneity of a platinum surface partially covered with methanol adsorption products. In contrast to the double-layer CPE, the CPE for adsorption of hydrogen was not affected significantly by the presence of methanol.

The charge-transfer resistance, R_{ct}, is the circuit element in Figure 6b that provides quantitative information about the kinetics of hydrogen adsorption and hence, how the adsorption and reaction of methanol affects the kinetics of hydrogen adsorption. From eq A-12 in the appendix, the inverse charge-transfer resistance is given as

$$R_{ct}^{-1} = F\left(\frac{\partial r_{ct}}{\partial E}\right)_{\theta_H} \tag{10}$$

where θ_H is the coverage of the electrode with hydrogen. The adsorption of hydrogen (upd) may be written as

$$H^+(aq) + e^- \underset{k_{-1}}{\overset{k_1}{\leftrightarrow}} H(ads) \tag{11}$$

In the presence of blocking species such as methanol adsorption products, the rate of charge transfer is

$$r_{ct} = \frac{N}{N_A}\{k_{-1}\theta_H \exp[(1-\beta)fE] - k_1(1-\theta_H-\theta_I)c_{H^+}\exp[-\beta fE]\} \tag{12}$$

where k_1 and k_{-1} are the rate constants for adsorption and desorption, respectively, θ_I is the coverage of the blocking species, c_{H^+} is the bulk concentration of hydrogen ions, β is the charge-transfer coefficient, and f is defined as F/RT. This rate expression assumes Butler−Volmer kinetics and a Langmuir adsorption isotherm.[44] The exchange rate constant may be defined as

$$k_0 \equiv k_1 c_{H^+}\exp[-\beta f E_{0.5}] = k_{-1}\exp[(1-\beta)fE_{0.5}] \tag{13}$$

where $E_{0.5}$ is the electrode potential at a steady-state coverage of half of the unblocked sites being covered with hydrogen (i.e., $\theta_H = 0.5(1-\theta_I)$). The rate of charge transfer then becomes

$$r_{ct} = k_0\frac{N}{N_A}\{\theta_H \exp[(1-\beta)f(E-E_{0.5})] - (1-\theta_H-\theta_I)\exp[-\beta f(E-E_{0.5})]\} \tag{14}$$

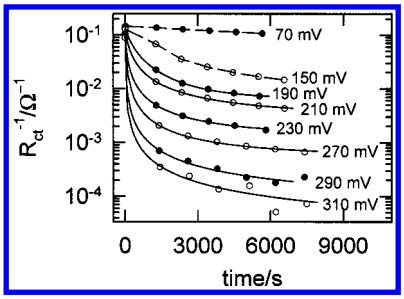

Figure 7. Inverse charge-transfer resistance for adsorption of hydrogen obtained from fits of the data to the equivalent circuit in Figure 6b as a function of time and electrode potential. The solid lines represent fits to the kinetic model described in the text and the dashed lines are to guide the eye.

The steady-state coverage of hydrogen, which is in equilibrium with available adsorption sites, may be expressed as

$$\theta_H = \frac{1-\theta_I}{1+\exp[f(E-E_{0.5})]} \tag{15}$$

Equations 10, 14, and 15 lead to an inverse charge-transfer resistance of

$$R_{ct}^{-1} = Fk_0 f(1-\theta_I)\left(\frac{N}{N_A}\right)\frac{\exp[(1-\beta)f(E-E_{0.5})]}{1+\exp[f(E-E_{0.5})]} \tag{16}$$

the key result being that the inverse charge-transfer resistance at a given electrode potential is proportional to the fraction of sites not blocked by methanol adsorption products. Thus, the coverage of methanol adsorption products can be monitored as a function of time by measuring the inverse charge-transfer resistance as a function of time.

Shown in Figure 7 is the inverse charge transfer resistance plotted as a function of the start time for the impedance scan at various potentials in the region of upd hydrogen. At low potentials in the region of weakly adsorbed hydrogen (i.e., 70 mV in Figure 7) the inverse charge transfer resistance does not change significantly, indicating negligible adsorption of methanol. As the potential is increased to the most positive potentials of the region corresponding to weakly adsorbed hydrogen (i.e., 150 mV in Figure 7) the inverse charge-transfer resistance decreases due to increasing coverage of the electrode surface with methanol adsorption products. The buildup of methanol adsorption products, however, is slow at 150 mV, which is indicated by the 1 order of magnitude decrease in the inverse charge-transfer resistance at 6000 s. This result is consistent with IR and radiotracer experiments, which indicate that significant amounts of adsorbed CO is not detected during the electro-oxidation of methanol until about 200 mV.[7,10,11,24] Chandrasekaran et al. detected two types of adsorbed CO during the electro-oxidation of methanol, one that they attributed to linear-bonded CO and a second that they attributed to bridge-bonded CO.[10] The linear-bonded CO was present only at potentials roughly corresponding to the region of weakly adsorbed hydrogen. The bridge-bonded CO, which attained much higher coverages than the linear-bonded CO, became detectable at 200 mV. It is possible that the slow formation of methanol adsorption products indicated by impedance spectroscopy within the region of weakly adsorbed hydrogen corresponds to the slow buildup of linear-bonded CO detected by IR. As the potential is increased into the region of strongly adsorbed hydrogen (i.e., 310 mV in Figure 7), the value of the inverse charge-transfer resistance decreases more rapidly, drop-

ping over 3 orders of magnitude after 6000 s. These results are consistent with the series capacitance data (Figure 2), which indicates high coverages of methanol adsorption products in the region of strongly adsorbed hydrogen.

Starting at 190 mV, there is also a change in the profile of the inverse charge-transfer resistance versus time curve. At short times and potentials ≥190 mV, the inverse charge transfer resistance decreases more rapidly than in the region of weakly adsorbed hydrogen (e.g., compare 150 and 190 mV in Figure 7). At longer times and potentials ≥190 mV, the inverse charge transfer resistance appears to approach an asymptotic value while at lower potentials, there appears to be a continuing exponential decrease (e.g., compare 150 and 190 mV in Figure 7). The differences in the behavior of the inverse charge transfer resistance between the regions of weakly adsorbed hydrogen and strongly adsorbed hydrogen add to the previously discussed results (Figures 1−3), which indicate a change in the mechanism of the methanol reaction between these two regions.

The coverage of methanol adsorption products is related to the inverse charge transfer resistance for adsorption of hydrogen (eq 16), and therefore, can be fit to models that describe the kinetics of formation of methanol adsorption products. Attempts to fit the inverse charge transfer resistance to a consistent model at potentials less than 190 mV were unsuccessful. Data obtained at potentials between 190 and 310 mV were fitted successfully and are plotted in Figure 7. The model that consistently fits the data includes (a) an adsorption term where the rate of formation of adsorbate is proportional to the fraction of free metal sites and (b) a desorption or oxidation term where the rate of removal of adsorbate is proportional to the fraction of free metal sites and the coverage of the adsorbate. The oxidative removal of methanol adsorption products requires the reaction of the adsorbate with an oxygen containing species. This oxygen containing species may be in the form of adsorbed OH,[4,5] adsorbed H_2O,[14,16,49] or hydrous oxides.[17−22] At least in the case of adsorbed OH or H_2O, the formation of the oxygen containing species requires free metal sites and thus the rate of removal of adsorbate will be proportional to the fraction of these metal sites. The electro-oxidation of methanol will then be given by

$$CH_3OH \xrightarrow{k_a} I \xrightarrow{k_d} \text{product} \qquad (17)$$

where k_a is the rate constant for adsorption rate, k_d is the rate constant for desorption or oxidation, and I is the methanol adsorption product, which can be considered a reaction intermediate at potentials ≥190 mV. The chemical nature of the intermediate and the product is irrelevant to the mathematics of the model. The differential equation describing the model used is given by

$$\frac{d\theta_I}{dt} = k_a(1 - \theta_H - \theta_I) - k_d(1 - \theta_H - \theta_I)\theta_I \qquad (18)$$

The solution of this differential equation along with eq 15 gives the coverage of the intermediate as a function time as

$$\theta_I = \frac{1 - \exp\left[\frac{\exp[f(E - E_{0.5})]}{1 + \exp[f(E - E_{0.5})]}(k_d - k_a)t\right]}{1 - \frac{k_d}{k_a}\exp\left[\frac{\exp[f(E - E_{0.5})]}{1 + \exp[f(E - E_{0.5})]}(k_d - k_a)t\right]} \qquad (19)$$

This equation can be used in eq 16 to obtain the inverse charge-transfer resistance as a function of time, which can then be fit to the data.

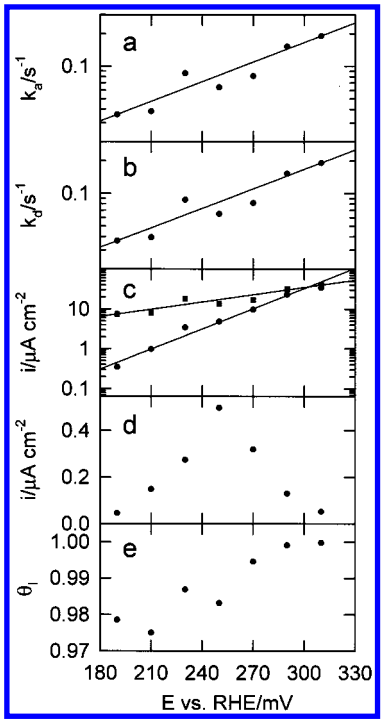

Figure 8. Kinetic parameters obtained from the fits of the inverse charge transfer resistance for hydrogen adsorption to the kinetic model described in the text. (a) Rate constant for adsorption/dehydrogenation of methanol. (b) Rate constant for oxidative removal of the blocking intermediate. (c) Initial current density associated with the adsorption of methanol before (circles) and after (squares) correcting for hydrogen coadsorption. The lines represent fits to Tafel lines. (d) Current density at steady-state for the oxidation of methanol. (e) Steady-state coverage of blocking intermediates at sites for strongly adsorbed hydrogen.

In performing the fits, β was assumed to be 0.5, T was set at 298 K, and $E_{0.5}$ was obtained from the peak in the cyclic voltammogram that corresponds to strongly adsorbed hydrogen, and was measured in each experiment prior to injecting methanol. The value for the number of surface atoms, N, was obtained in the usual manner by integrating the peaks corresponding to desorption of hydrogen in the cyclic voltammogram. Since the fits were performed in the region of strongly adsorbed hydrogen, only those sites were probed and thus the coverage of methanol adsorption products, θ_I, refers to the coverage of those sites. The moles of sites available for strongly adsorbed hydrogen, N/N_f, was found to be 6.8×10^{-11} mol. From the fits, the average rate constant for the exchange of adsorbed hydrogen, k_0, in the region of strongly adsorbed hydrogen was found to be $9.4 \times 10^3\ s^{-1}$, which is on the order of previously found values.[26,43] Using this value for k_0, fitting of the data provided values for the rate constants for adsorption (k_a) and desorption (k_d) of methanol, which are plotted in Figure 8a,b, respectively. Both rate constants fit exponentials where k_a and k_d have Tafel slopes of 165 and 167 mV/decade, respectively. The initial current for adsorption at each potential can be calculated using

$$i_a = F\frac{N}{N_A}k_a\frac{\exp[f(E - E_{0.5})]}{1 + \exp[f(E - E_{0.5})]} \qquad (20)$$

assuming that the initial adsorption process is a one electron process as indicated approximately by the Tafel slope of k_a. The initial currents for adsorption obtained from eq 20 are plotted in Figure 8c. The predicted Tafel slope for the initial current for adsorption was found to be 59.3 mV/decade. Because

of the relatively small currents generated by the methanol reaction in the region of adsorbed hydrogen, few reports exist in the literature that describe data measured in this potential region.[2] Bagotzky and Vassilyev found a Tafel slope of 135 mV/decade in the region of adsorbed hydrogen.[4] Their data, however, were not corrected for the non-steady-state current generated by the adsorption of hydrogen at short times, which could account for the discrepancy with our results. In addition, their results were obtained by stepping the electrode from high potentials instead of stepping the electrode from low potentials, where adsorption of methanol is negligible. Note that in conjunction with the results that we obtained in the double-layer region, this result indicates that the measured Tafel slope should change from 59.3 mV/decade in the hydrogen region to 106 mV/decade in the double-layer region. An abrupt change in the Tafel slope between the hydrogen adsorption and double-layer regions was reported by Bagotzky and Vassilyev.[4] Their reported values, however, are approximately a factor of 2 larger than the values we obtained. The predicted Tafel slope of 59.3 mV/decade in the hydrogen adsorption region does not represent the kinetics of methanol adsorption since the coverage of hydrogen, and hence the coverage of free metal sites initially available, depend on the potential of the electrode. The initial current for adsorption corrected for the coverage of hydrogen is shown in Figure 8c and as expected, yields the same Tafel slope as k_a, 165 mV/decade. This slope is slightly higher than the Tafel slope of 128 mV/decade measured at potentials just positive of the hydrogen adsorption region.[15]

Steady-state kinetic information also can be obtained from the fit parameters. By setting eq 18 equal to zero, the steady-state coverage of the intermediate in the methanol reaction is given by

$$\theta_{\mathrm{Iss}} = \frac{k_a}{k_d} \tag{21}$$

and the steady-state current is given by

$$i_{\mathrm{SS}} = 6F\frac{N}{N_A}k_a\frac{\exp[f(E - E_{0.5})](1 - \theta_{\mathrm{Iss}})}{\exp[f(E - E_{0.5})] + \theta_{\mathrm{Iss}}} \tag{22}$$

assuming that methanol is oxidized completely to CO_2 and thus a six electron process. The steady-state current is plotted in Figure 8d. The low values predicted for the steady-state current explains why currents associated with the oxidation of methanol in the region of adsorbed hydrogen are not measurable. A peak in the steady state current occurs at approximately the same potential that the peak due to strongly adsorbed hydrogen occurs in the cyclic voltammogram when methanol is absent (Figure 1c). In addition, the predicted peak is at the same potential (i.e., 250 mV) that a peak due to the methanol reaction is observed during the first cyclic voltammetry sweep in the presence of methanol.[7,8,12,25]

Figure 8e shows the predicted steady-state coverage of the intermediate. The predicted coverage is very high and increases with increasing potential, approaching one at the higher potentials of the hydrogen adsorption region. While there is no agreement in the literature on the maximum coverage of the blocking intermediate in the hydrogen adsorption region, several studies report high coverages in this region and the increasing trend with increasing potential is always observed.[5,10,50,51] Previous studies reporting coverages much lower than predicted here probably represent non steady-state conditions. For example, using the model of eq 19 and the fit parameters, a value of 0.696 is obtained for θ_I at 250 mV after 100 s as compared to the steady-state value of 0.983.

4. Discussion

The potential dependence of the four physical impedance parameters obtained from the impedance data for the electro-oxidation of methanol indicates five potential regions between 40 and 800 mV where there is a change in the mechanism for the electro-oxidation of methanol (Figure 5). The impedance data for the adsorption of hydrogen in the presence of methanol also indicates a change in the mechanism for the electro-oxidation of methanol between the two lowest potential regions (those corresponding to the region of weakly and strongly adsorbing hydrogen respectively). These five potential regions will be discussed in turn.

4.1. Electrode Potentials 40−200 mV. At potentials more negative than 230 mV, charge transfer due to the electro-oxidation of methanol is not detected by impedance spectroscopy as is evident by the absence of a semicircle in the complex plane at low frequencies. The decay in the inverse charge-transfer resistance for the adsorption of hydrogen (Figure 7) indicates that methanol adsorbs at these potentials. The adsorption of methanol, however, is slow enough that charge transfer is not observed. The formation of methanol adsorption products is slow because of the low overpotential and the high coverage of adsorbed hydrogen. The inability to fit the profiles of the inverse charge-transfer resistance for the adsorption of hydrogen to a model that includes the removal of adsorbate indicates that oxidative removal of methanol adsorption products does not occur at these potentials. This conclusion is further supported by the nonasymptotic behavior of the inverse charge-transfer resistance. It is reasonable to assume that at these potentials, there is no source of reactive oxygen to effect the removal of the methanol adsorption products.

4.2. Electrode Potentials 200−370 mV. At potentials higher than 200 mV, the rate at which methanol is electro-oxidized is enhanced, which is indicated by the detection of a charge transfer semicircle in the low frequency region of the impedance spectrum (Figure 3a). We believe this enhancement is due to the oxidative removal of methanol adsorption products, which means that the methanol adsorption products at these potentials are adsorbed reaction intermediates. It has been proposed previously that any current due to the electro-oxidation of methanol observed in the hydrogen adsorption region is due only to the formation of methanol adsorption products (i.e., dehydrogenation of methanol) without the oxidative removal of the adsorbates formed.[7,24] The successful fitting of the profiles shown in Figure 7 to a model that includes oxidative removal of the methanol adsorption products (eq 17) indicates the presence of a reactive oxygen source. The potentials in this region are too low for the presence of any adsorbed OH (the usually cited source of oxygen for the electro-oxidation of methanol). Burke et al. has proposed that incipient hydrous oxides may be present and active at potentials as low as 200 mV.[17−22] One study using a thermally activated platinum electrode revealed a large peak due to oxide formation in the cyclic voltammogram at 200 mV.[22] Adsorbed water is another possibility for the source of oxygen and has been detected by infrared spectroscopy at these low potentials.[11,52,53]

The kinetic parameters for the formation and removal of the adsorbed reaction intermediate (Figure 8a,b) in this potential region indicate that both processes are activated by potential and have Tafel slopes of about 165 mV/decade. Similar to what has been observed previously, this result indicates that the rate-

limiting steps in both the formation of the adsorbed intermediate and its removal are one-electron events.[15] The kinetic parameters predict the presence of a peak in the steady-state current (Figure 8d). The source of this peak is the buildup of the methanol reaction intermediate, which further inhibits the adsorption of methanol (Figure 8e). These results indicate that the presence of a current peak at these potentials observed during the first CV scan[7,8,12,24,25] is not a transient effect and is due to dehydrogenation of methanol *and* oxidation of the adsorbed intermediate as opposed to dehydrogenation alone.

The inverse charge transfer resistance for the electro-oxidation of methanol decreases slightly with potential in this potential region (Figure 5). Without the effect of changes in the coverage of intermediates, the inverse charge transfer resistance depends only on kinetic parameters, which are increasing exponentially (Figure 8). Therefore, the decrease in inverse charge-transfer resistance is due to increasing coverage of intermediates (Figure 8e).

Interestingly, the two lowest potential regions for the electro-oxidation of methanol coincide with the potentials for the two states of hydrogen adsorption. It is possible that the adsorption sites for strongly adsorbed hydrogen adsorb oxygen species at low potentials while the weakly adsorbed hydrogen sites do not. If this were the case, the oxidative removal of the adsorbed reaction intermediate could not commence until the strongly adsorbed hydrogen began to desorb. Another possibility is that reactive oxygen species formed at low potentials are formed at a potential of about 200 mV and thus, activation of the electro-oxidation of methanol coinciding with strong hydrogen adsorption is only coincidental. Burke et al. proposed the formation of an active hydrous oxide species that they labeled HO2 at about 200 mV and related its formation to the small anodic peak observed in the cyclic voltammogram between the peaks for weakly and strongly adsorbed hydrogen.[17,19] The source of the small anodic peak at 200 mV is controversial. In addition to the proposed hydrous oxide, proposals for the source of the 200 mV peak include the desorption of hydrogen from crystal grain edges, hydrogen-anion interaction, hydrogen adsorption on Pt(111) sites, hydrogen absorption, and dihydrogen adsorption.[54,55]

4.3. Electrode Potentials 370−580 mV. At 370 mV, the inverse charge transfer resistance begins to increase exponentially (Figure 5a) indicating that the coverage stops changing significantly with potential, allowing the inverse charge-transfer resistance to follow the exponential increase in the kinetics of formation and removal of the adsorbed intermediate. The Tafel slopes of the inverse charge-transfer resistance and inverse faradaic resistance of 108 mV/decade and 106 mV/decade, respectively, indicate that the rate-limiting steps are one electron processes. The change in the rate at which methanol is electro-oxidized at 370 mV can be explained by a further activation in the oxidative removal of the adsorbed reaction intermediate, which would cause the coverage of the reaction intermediate to stop increasing with potential.

As was mentioned previously, the inverse coverage resistance is positive (Figure 5b) indicating that the change in coverage caused by a change in potential increases the rate of reaction. At these potentials, increasing the coverage decreases the current as is evidenced by current that decays with time.[2,4,12−14] Consequently, it is reasonable to conclude that the positive value for the inverse coverage resistance indicates that the intermediate coverage is decreasing with increasing potential. The rate of decrease in coverage of the intermediate is small based on the exponential increase of the inverse charge transfer resistance because if the rate of decrease in coverage were large, the inverse charge transfer resistance would increase faster than the exponential increase of the kinetic parameters. Using this same reasoning, the inverse coverage resistance can be predicted to be negative at lower potentials where the intermediate coverage is increasing. A negative inverse coverage resistance indicates that the second semicircle in the complex plane would be located in the first quadrant, revealing capacitive behavior. Thus, there should be a transition of the second semicircle in the complex plane from capacitive behavior to inductive behavior as the potential is increased and the intermediate coverage stops increasing and begins to decrease. At potentials below 470 mV, the effects of a second semicircle within the frequency range that could be measured were not significant enough to include in the data fitting. The small effect that the second semicircle has on the phase of impedance at low frequency, however, could be detected. From 370 to 470 mV, the phase of the impedance measured at 0.06 Hz decreases rapidly (Figure 1a). This decrease indicates the transition of the low-frequency impedance from capacitive to inductive behavior.

The exponential increase in the inverse coverage resistance in this potential region is another indication that the intermediate coverage is not changing significantly with potential. Intermediate coverage that is changing slowly as a function of potential will give rise to a constant $d\theta/dE$. Thus, the inverse coverage resistance will depend primarily on $(\partial r_{ct}/\partial\theta)_E$ (see Table 1), which will follow the exponential increase of the kinetic parameters.

The chemical nature of the oxygen species formed at 370 mV probably is not adsorbed OH considering the low potentials. The presence of a reactive oxygen species distinct from adsorbed OH is supported by the preoxidation peak observed at these potentials under certain conditions during the oxidation of carbon monoxide.[56] Burke et al. have proposed the presence of a second hydrous oxide species that they labeled HO1 at these potentials.[18−21] If the oxygen source is adsorbed water, it is interesting to note that an abrupt shift in the IR peak associated with adsorbed water occurs at 350 mV on Pt(111), which has been attributed to a change in the orientation of water from an H-down to an O-down configuration. Presumably, the O-down configuration is the more active source of oxygen.[11,53] IR evidence also predicts an increasing O-down configuration with increasing potential on polycrystalline platinum based on peak areas. No evidence for a sudden transition, however, has been reported.[52] Further evidence for the adsorption of an oxygen containing species at about 370 mV is provided by Gamboa-Aldeco et al. in their study of the adsorption of bisulfate on platinum.[57] They found a peak in the bisulfate coverage on Pt(100) at 390 mV that they attributed to competitive adsorption between bisulfate and an adsorbed oxygen containing species. Furthermore, they proposed that adsorption of bisulfate on polycrystalline platinum can be demonstrated to be the superposition of adsorbed bisulfate on the different single crystal planes of platinum. It is therefore possible that the source of reactive oxygen that enhances the electro-oxidation of methanol at 370 mV is formed on Pt(100) sites.

4.4. Electrode Potentials 580−650 mV. Above 580 mV, the coverage relaxation time begins to decrease (Figure 5d). This decrease can be attributed to a further activation in the rate of removal of the adsorbed reaction intermediate, which would cause the intermediate coverage to decrease faster with increasing potential and thus effect a faster relaxation to equilibrium. Again, it seems unlikely that the newly formed source of oxygen is chemisorbed hydroxy. Burke et al. have demonstrated the

presence of platinum oxide at these potentials on electrodes activated by various potential and temperature treatments.[19−21] As with the lower potential hydrous oxides HO1 and HO2, they interpret this species as being formed by the oxidation of surface platinum to yield platinum adatoms of varying coordination numbers. Recently, it was demonstrated that there is a discontinuity in the rate of Stark tuning with respect to potential at about 500 mV during the electro-oxidation of methanol.[58] It is possible that this effect is related to the change in reaction mechanism indicated by impedance spectroscopy at 580 mV.

4.5. Electrode Potentials above 650 mV. At 650 mV, the inverse charge-transfer resistance, inverse coverage resistance, and inverse faradaic resistance reveal significant discontinuities (Figure 5). This drastic effect can be explained by the formation of chemisorbed hydroxy, which enhances the oxidative removal of the adsorbed intermediate and inhibits the formation of the intermediate by blocking adsorption sites. The inverse charge-transfer resistance and inverse coverage resistance decreases with increasing potential because the kinetic terms for the adsorption of methanol decrease due to inhibition as the coverage of hydroxy radicals increase. The inverse charge-transfer resistance passes through zero at 700 mV, indicating that the contributions of the processes for the formation and removal of the reaction intermediate are equal. Above 700 mV, the inverse charge-transfer resistance becomes negative, indicating that the formation of intermediate is inhibited enough to cause the rate of reaction to decrease with increasing potential if the coverage of the intermediate is held constant. Experimentally, however, the rate of reaction begins to *increase* at 700 mV (Figure 1c), indicating that the reaction is driven by a rapidly decreasing coverage of intermediate with increasing potential. The increasing rate of reaction with increasing potential is indicated by the fact that the inverse faradaic resistance is positive. Because the inverse faradaic resistance is the sum of the inverse charge-transfer resistance and the inverse coverage resistance (eq 7), a positive inverse faradaic resistance indicates that the contribution due to coverage (inverse coverage resistance) is greater than the contribution due to kinetics (inverse charge-transfer resistance).

The presence of a zero charge-transfer resistance at 700 mV indicates that potential oscillations are possible and the presence of a negative charge-transfer resistance above 700 mV indicates that current oscillations are possible.[59,60] Galvanostatic experiments that we have conducted as well as a previous report[9] on potential oscillations during the electro-oxidation of methanol indicate that potential oscillations occur near 700 mV, a potential predicted by impedance spectroscopy. We also have observed current oscillations during potentiostatic experiments.[61]

4.6. Source of Mechanistic Changes. The changes in the mechanism for the electro-oxidation of methanol indicated by the changes in the impedance parameters between 40 and 800 mV are hypothesized to be due to changes in the state of the platinum surface. At each region of higher potential, the platinum surface becomes more active for the transfer of an oxygen containing species to the chemisorbed methanol adsorption products. Each potential region is therefore characterized by a different state of oxygen activation, yielding mechanisms for the electro-oxidation of methanol that include these states.

4.7. Impedance Spectroscopy vs Cyclic Voltammetry. Impedance measurements of the charge transfer associated with the electro-oxidation of methanol in the region of strongly adsorbed hydrogen and the peak in current predicted at steady-state (Figure 8d) coincide with the peak observed in the first cyclic voltammogram scanned. Subsequent CV scans do not reveal any features in the hydrogen region due to the buildup of adsorbed reaction intermediates, and thus, make it difficult to obtain kinetic information at these potentials. The need for kinetic data at these low potentials was highlighted in a recent review.[2] We have demonstrated that impedance spectroscopy can provide this kinetic data. The change observed in the impedance data at 370 mV (Figure 5a) has a counterpart in cyclic voltammetry. This potential corresponds to the point where anodic current for the electro-oxidation of methanol is observed on the first scan[12] and where, even after the first scan, the current of the reverse scan of the CV decays to zero. Presumably, during the first scan and the reverse scans, the coverage of the electrode with the reaction intermediate is relatively low, allowing the oxidation current at 370 mV to be detected.

The change in the impedance at 580 mV for the electro-oxidation of methanol does not have a counterpart in cyclic voltammetry. The change observed at 650 mV, however, corresponds to an accelerated current for the electro-oxidation of methanol measured during the forward scan of the cyclic voltammogram. This acceleration is due to the rapidly decreasing coverage of intermediate caused by the formation of chemisorbed hydroxy radicals that are highly reactive. The current peak on the reverse scan of the cyclic voltammogram is located at about 700 mV, corresponding to the potential where the inverse charge transfer resistance is zero and where potential oscillations can occur. On the reverse scan, the intermediate coverage initially is zero because the electrode is saturated with chemisorbed hydroxy. Thus, the current will not be affected as much by changes in the coverage of intermediates. Without a contribution from changes in the coverage of intermediate, the current in the reverse scan of the CV will be determined largely by the reaction kinetics. Consequently, the current in the CV follows the trends indicated by the inverse charge-transfer resistance, which predicts a peak (zero slope) at 700 mV.

4.8. Parallel vs Serial Mechanism. There has been considerable debate over whether the mechanism for the electro-oxidation of methanol follows a serial mechanism, going through a slow intermediate, or a parallel mechanism, which includes the serial path plus a path consisting of reactive intermediates that do not have an appreciable lifetime.[2,6,13,50,51,62−65] In addition to a parallel path leading to the same product, evidence of reaction paths that oxidize methanol to formaldehyde without an adsorbed intermediate has been reported recently.[66,67] Unfortunately, as is illustrated in eq A-1, impedance spectroscopy cannot answer this question. In this paper, the impedance results have been discussed in terms of a serial mechanism. If there are significant parallel paths present, however, the charge transfer derivatives in the inverse charge transfer, inverse coverage, and inverse faradaic resistances will include terms for the parallel mechanisms. The charge transfer derivatives for both parallel and serial pathways depend similarly on potential and coverage of the intermediate formed in the serial pathway. This similar dependence arises from the fact that the coverage of reactive intermediates on the electrode surface is negligible in the parallel pathways. The coverage term in the impedance model, θ, refers only to the coverage of the intermediate in the serial mechanism, even when parallel pathways are present. Increasing the coverage of the intermediate will have the same effect on both the serial or parallel mechanism—that is, the formation of additional adsorbed intermediate and adsorbed oxygen containing species is inhibited because active sites are blocked. Likewise, increasing the potential of the electrode will have the same effect on both the serial and parallel mechanisms

by creating an electrode surface that is more reactive for adsorbed intermediate formation and oxidation of those intermediates. It is reasonable to assume that the reactive oxygen containing species that oxidatively remove the intermediate in the serial mechanism also will remove the intermediates in the parallel mechanism.

Unfortunately, if parallel pathways are present during the electro-oxidation of methanol, they cannot be investigated using impedance spectroscopy unless their adsorbed intermediates achieved a significant enough coverage to be detected. Detectable parallel pathways would be indicated by impedance spectra containing three or more semicircles in the complex plane (i.e., two or more total adsorbed intermediates). At the very least, the impedance results indicate that the serial mechanism is active at all potentials starting in the region of strongly adsorbed hydrogen.

It has been proposed that if both serial and parallel pathways are present, there may be time dependent competition between them.[64] This proposal should not affect our conclusions for the following reasons: (i) These time dependent effects have been observed primarily at reaction times of less than 10 s.[64] Our impedance measurements were commenced after 30 s. (ii) The principle change with reaction time is the build up of the serial intermediate. As discussed above, a change in the coverage of the serial intermediate coverage affects both serial and parallel pathway impedance parameters the same. (iii) The time dependence of the impedance spectra does not indicate a mechanistic change with time for reaction times longer than 30 s.[68]

5. Conclusions

Impedance spectroscopy of the electro-oxidation of methanol on smooth polycrystalline platinum indicates that the reaction proceeds with one adsorbed intermediate of appreciable surface concentration and lifetime. The turnover of all other intermediates is too fast to be detected. IS first detects charge transfer due to the electro-oxidation of methanol at about 200 mV. Impedance spectra were fit to an equivalent circuit that models a reaction with one adsorbed intermediate to obtain physical impedance parameters as a function of potential. The trends in the impedance parameters indicate the presence of five potential regions where the mechanism changes for the electro-oxidation of methanol. The mechanistic changes can be interpreted in terms of the formation of four different reactive oxygen species with increasing activity toward the removal of the adsorbed reaction intermediate with increasing potential. The impedance parameters also predict how the coverage of the reaction intermediate changes with potential.

At low potentials, the impedance response due to adsorption of hydrogen can be detected. Because the buildup of methanol reaction intermediates occupy sites for adsorption of hydrogen, the impedance response for adsorption of hydrogen can be used as an in situ probe to monitor the buildup of reaction intermediates with time. Fitting of the inverse charge transfer resistance for adsorption of hydrogen versus time data to a model that describes the buildup of intermediate provides kinetic information about the electro-oxidation of methanol at low potentials. The information obtained indicates that only the formation of methanol adsorption products occurs in the region of weakly adsorbed hydrogen and that oxidative removal of these adsorbates commences in the region of strongly adsorbed hydrogen.

This study demonstrates that impedance spectroscopy is a powerful technique with which to study the kinetics and mechanism of the electro-oxidation of methanol. Further applications of this technique to the methanol reaction under different conditions (i.e., varying catalyst, electrolyte, and temperature) as well other organic electro-oxidation systems should prove fruitful. In addition, this study identifies five states in the mechanism for the electro-oxidation of methanol that arise from the formation of different sources of reactive oxygen. Further study of these sources of oxygen could provide insight into improving the rate of reaction at low potentials and thus, improving the performance of direct methanol fuel cells.

Appendix

The general derivation of the impedance for reactions containing adsorbed intermediates or adsorbed reactants/products has been reported previously[31−35] as has derivations for a few specific cases.[45,69,70] The derivation presented here is similar to these reports and the result is identical. This derivation applies to any reacting system that contains one adsorbed intermediate. A multiplicity of possible pathways and parallel reactions does not affect the result. A general reaction scheme may be presented as

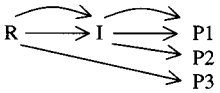

(A-1)

where R is the reactant, I is the adsorbed intermediate, and P1, P2, and P3 are possible products. This scheme is by no means the limit of the number of possible reaction pathways and products. An infinite number of such pathways and products would lead to the same results as long as only one adsorbed intermediate was involved. The overall charge-transfer rate will be the sum of each charge-transfer step,

$$r_{ct} = \sum_i n_i r_{cti} \tag{A-2}$$

where n_i is the number of electrons transferred in each step. A perturbation in the applied potential, ΔE, will result in a corresponding perturbation in the rate of charge transfer, Δr_{ct}. If this perturbation is small, higher order terms in the Taylor series expansion will be negligible, and a linear response is expected. This linear response, along with the fact that the rate of charge transfer will depend on the intermediate coverage, θ, and electrode potential, E, leads to

$$\Delta r_{ct} = \left(\frac{\partial r_{ct}}{\partial \theta}\right)_E \Delta\theta + \left(\frac{\partial r_{ct}}{\partial E}\right)_\theta \Delta E \tag{A-3}$$

for the resulting perturbation in the rate of charge transfer. A perturbation in potential will lead to a similar linear perturbation in the rate of change in the coverage of the intermediate, r_θ, leading to

$$\Delta r_\theta = \left(\frac{\partial r_\theta}{\partial \theta}\right)_E \Delta\theta + \left(\frac{\partial r_\theta}{\partial E}\right)_\theta \Delta E \tag{A-4}$$

The perturbation in the rate of change in the coverage may be expressed further as

$$\Delta r_\theta \equiv \frac{N\, \mathrm{d}\Delta\theta}{N_A\, \mathrm{d}t} = \frac{N}{N_A} s\Delta\theta \tag{A-5}$$

via Laplace transformation where the Laplace variable, s, is given by $j\omega$ in the case of impedance spectroscopy. The number of adsorbed intermediates at full coverage is represented by N and N_A is Avogadro's constant. Equations A-3, A-4, and A-5

may be solved for Δr_{ct} yielding

$$\Delta r_{ct} = \frac{s\left(\frac{\partial r_{ct}}{\partial E}\right)_\theta + \frac{N}{N_A}\left[\left(\frac{\partial r_\theta}{\partial E}\right)_\theta\left(\frac{\partial r_{ct}}{\partial \theta}\right)_E - \left(\frac{\partial r_{ct}}{\partial E}\right)_\theta\left(\frac{\partial r_\theta}{\partial \theta}\right)_E\right]}{s - \frac{N}{N_A}\left(\frac{\partial r_\theta}{\partial \theta}\right)_E}\Delta E \tag{A-6}$$

The perturbation in the measured current is related to Δr_{ct} by

$$\Delta i = F\Delta r_{ct} \tag{A-7}$$

where F is Faraday's constant. The resulting impedance of the electrode is given by

$$Z \equiv \frac{\Delta E}{\Delta i} = \left(\frac{1}{F}\right)\frac{s - \frac{N}{N_A}\left(\frac{\partial r_\theta}{\partial \theta}\right)_E}{s\left(\frac{\partial r_{ct}}{\partial E}\right)_\theta + \frac{N}{N_A}\left[\left(\frac{\partial r_\theta}{\partial E}\right)_\theta\left(\frac{\partial r_{ct}}{\partial \theta}\right)_E - \left(\frac{\partial r_{ct}}{\partial E}\right)_\theta\left(\frac{\partial r_\theta}{\partial \theta}\right)_E\right]} \tag{A-8}$$

This impedance is equivalent to a resistor in series with a parallel combination of a resistor and a capacitor. This circuit is known as the Armstrong circuit.[69] The equivalent circuit of Figure 4b is obtained when the impedance for the double layer and solution resistance are included. The parameters of the faradaic branch in the circuit are given by

$$R_{ct} = \frac{1}{F\left(\frac{\partial r_{ct}}{\partial E}\right)_\theta}$$

$$R_1 = \frac{1}{F}\frac{\left(\frac{\partial r_\theta}{\partial E}\right)_\theta\left(\frac{\partial r_{ct}}{\partial \theta}\right)_E}{\left(\frac{\partial r_{ct}}{\partial E}\right)_\theta}\left[\left(\frac{\partial r_{ct}}{\partial E}\right)_\theta\left(\frac{\partial r_\theta}{\partial \theta}\right)_E - \left(\frac{\partial r_\theta}{\partial E}\right)_\theta\left(\frac{\partial r_{ct}}{\partial \theta}\right)_E\right]^{-1}$$

$$C_1 = F\frac{N}{N_A}\frac{\left(\frac{\partial r_{ct}}{\partial E}\right)_\theta^2}{\left(\frac{\partial r_\theta}{\partial E}\right)_\theta\left(\frac{\partial r_{ct}}{\partial \theta}\right)_E} \tag{A-9}$$

In the case of hydrogen adsorption (eq 11), the product is the adsorbed species and there is only one pathway present. Equation A-1 then reduces to

$$\mathrm{R} \rightarrow \mathrm{I} \tag{A-10}$$

where I is now the adsorbed product. In this case the rate of charge transfer will equal the rate of change of the coverage, $r_{ct} = r_\theta$, and eq A-8 reduces to

$$Z = \left(\frac{1}{F}\right)\frac{s - \frac{N_A}{N}\left(\frac{\partial r_{ct}}{\partial \theta}\right)_E}{s\left(\frac{\partial r_{ct}}{\partial E}\right)_\theta} \tag{A-11}$$

This impedance is equivalent to a resistor in series with a capacitor. When combined with the impedance for the double layer and the solution resistance, the equivalent circuit in Figure 6b is obtained with the exception that in Figure 6b, the series capacitor has been replaced with a CPE. The circuit elements in the faradaic branch of Figure 6b (using a capacitor instead of the CPE) are given by

$$R_{ct} = \frac{1}{F\left(\frac{\partial r_{ct}}{\partial E}\right)_\theta}$$

$$C_a = F\frac{N}{N_A}\frac{\left(\frac{\partial r_{ct}}{\partial E}\right)_\theta}{\left(\frac{\partial r_{ct}}{\partial \theta}\right)_E} \tag{A-12}$$

Acknowledgment. G.T.R.P. is a recipient of a CAREER award from the National Science Foundation and is grateful for generous support from the University of California Energy Institute, NSF, ONR, DOE and Sandia National Laboratories. R.E.M. is grateful for pre-doctoral fellowships awarded through NSF-IGERT and DOE-GATE programs.

References and Notes

(1) Parsons, R.; VanderNoot, T. *J. Electroanal. Chem.* **1988**, *257*, 9.
(2) Jarvi, T. D.; Stuve, E. M. Fundamental Aspects of Vacuum and Electrocatalytic Reactions of Methanol and Formic Acid on Platinum Surfaces. In *Electrocatalysis*; Lipkowski, J., Ross, P. N., Eds.; Wiley-VCH: New York, 1998; p 75.
(3) Muller, J. T.; Urban, P. M.; Holderich, W. F. *J. Power Sources* **1999**, *84*, 157.
(4) Bagotzky, V. S.; Vassilyev, Y. B. *Electrochim. Acta* **1967**, *12*, 1323.
(5) Bagotzky, V. S.; Vassiliev, Y. B.; Khazova, O. A. *J. Electroanal. Chem.* **1977**, *81*, 229.
(6) Sriramulu, S.; Jarvi, T. D.; Stuve, E. M. *J. Electroanal. Chem.* **1999**, *467*, 132.
(7) Markovic, N. M.; Gasteiger, H. A.; Ross, P. N. *Electrochim. Acta* **1995**, *40*, 91.
(8) Gasteiger, H. A.; Markovic, N.; Ross, P. N.; Cairns, E. J. *Electrochim. Acta* **1994**, *39*, 1825.
(9) Krausa, M.; Vielstich, W. *J. Electroanal. Chem.* **1995**, *399*, 7.
(10) Chandrasekaran, K.; Wass, J. C.; Bockris, J. O. M. *J. Electrochem. Soc.* **1990**, *137*, 518.
(11) Iwasita, T.; Xia, X. H.; Liess, H. D.; Vielstich, W. *J. Phys. Chem. B* **1997**, *101*, 7542.
(12) Gasteiger, H. A.; Markovic, N.; Ross, P. N.; Cairns, E. J. *J. Phys. Chem.* **1993**, *97*, 12020.
(13) Franaszczuk, K.; Herrero, E.; Zelanay, A.; Wieckowski, A.; Wang, J.; Masel, R. I. *J. Phys. Chem.* **1992**, *96*, 8509.
(14) Herrero, E.; Franaszczuk, K.; Wieckowski, A. *J. Phys. Chem.* **1994**, *98*, 8, 5074.
(15) Wieckowski, A.; Sobkowski, J. *J. Electroanal. Chem.* **1975**, *63*, 365.
(16) Schell, M. *J. Electroanal. Chem.* **1998**, *457*, 221.
(17) Burke, L. D.; Healy, J. F.; O'Dwyer, K. J.; O'Leary, W. A. *J. Electrochem. Soc.* **1989**, *136*, 1015.
(18) Burke, L. D.; Casey, J. K. *Electrochim. Acta* **1992**, *37*, 1817.
(19) Burke, L. D.; Buckley, D. T. *J. Appl. Electrochem.* **1995**, *25*, 913.
(20) Burke, L. D.; Buckley, D. T. *Russian J. Electrochem.* **1995**, *31*, 957.
(21) Burke, L. D.; Hurley, L. M. *Electrochim. Acta* **1999**, *44*, 3451.
(22) Burke, L. D.; Hurley, L. M. *J. Solid State Electrochem.* **2000**, *4*, 353.
(23) Macdonald, J. R. *LEVM*, 7.1 ed.; Solartron: Chapel Hill, NC, 1998.
(24) Xia, X. H.; Iwasita, T.; Ge, F.; Vielstich, W. *Electrochim. Acta* **1996**, *41*, 711.
(25) Morimoto, Y.; Yeager, E. B. *J. Electroanal. Chem.* **1998**, *444*, 95.
(26) Lasia, A. *Polish J. Chem.* **1995**, *69*, 639.
(27) Ohsaka, T.; Sawada, Y. *J. Electrochem. Soc.* **1975**, *123*, 1339.
(28) Luk'yanycheva, V. I.; Strochkova, E. M.; Bagotskii, V. S.; Knots, L. L. *Elektrokhimiya* **1971**, *7*, 267.
(29) Arico, A. S.; Kim, H.; Shukla, A. K.; Ravikumar, M. K.; Antonucci, V.; Giordano, N. *Electrochim. Acta* **1994**, *39*, 691.
(30) Mueller, J. T.; Urban, P. M. *J. Power Sources* **1998**, *75*, 139.
(31) Bai, L.; Conway, B. E. *Electrochim. Acta* **1993**, *38*, 1803.
(32) Harrington, D. A.; Conway, B. E. *Electrochim. Acta* **1987**, *32*, 1703.
(33) Wu, X.; Ma, H.; Chen, S. *J. Electrochem. Soc.* **1998**, *145*, 517.
(34) Wu, X.; Ma, H.; Chen, S.; Xu, Z.; Sui, A. *J. Electrochem. Soc.* **1999**, *146*, 8.
(35) Gabrielli, C.; Keddam, M. *Electrochim. Acta* **1996**, *41*, 957.
(36) Nyikos, L.; Pajkossy, T. *Electrochim. Acta.* **1985**, *30*, 1533.
(37) de Levie, R. *J. Electroanal. Chem.* **1990**, *281*, 1.
(38) Pajkossy, T. *J. Electroanal. Chem.* **1994**, *364*, 111.

(39) Brug, G. J.; Van Den Eeden, A. L. G.; Sluyters-Rehbach, M.; Sluyters, J. H. *J. Electroanal. Chem.* **1984**, *176*, 275.
(40) Kerner, Z.; Pajkossy, T. *J. Electroanal. Chem.* **1998**, *448*, 139.
(41) Baranski, A. S.; Krogulec, T.; Nelson, L. J.; Norouzi, P. *Anal. Chem.* **1998**, *70*, 2895.
(42) Glarum, S. H.; Marshall, J. H. *J. Electrochem. Soc.* **1979**, *126*, 424.
(43) Morin, S.; Dumont, H.; Conway, B. E. *J. Electroanal. Chem.* **1996**, *412*, 39.
(44) Oelgeklaus, R.; Rose, J.; Baltruschat, H. *J. Electroanal. Chem.* **1994**, *376*, 127.
(45) Sluyters-Rehbach, M.; Sluyters, J. H. A. C. Techniques. In *Electrodics: Experimental Techniques*; Yeager, E., Bockris, J. O. M., Conway, B. E., Sarangapani, S., Eds.; Plenum Press: New York, 1984; Vol. 9; p 259.
(46) Bai, L.; Gao, L.; Conway, B. E. *J. Chem. Soc., Faraday Trans.* **1993**, *89*, 235.
(47) Ekdunge, P.; Juttner, K.; Kreysa, G.; Kessler, T.; Ebert, M.; Lorenz, W. J. *J. Electrochem. Soc.* **1991**, *138*, 2660.
(48) Simpraga, R.; Bai, L.; Conway, B. E. *J. Appl. Electrochem.* **1995**, *25*, 628.
(49) Leiva, E. P. M.; Santos, E.; Iwasita, T. *J. Electroanal. Chem.* **1986**, *215*, 357.
(50) Corrigan, D. S.; Weaver, M. J. *J. Electroanal. Chem.* **1988**, *241*, 143.
(51) Wilhelm, S.; Iwasita, T.; Vielstich, W. *J. Electroanal. Chem.* **1987**, *238*, 383.
(52) Habib, M. A.; Bockris, J. O. M. *Langmuir* **1986**, *2*, 388.
(53) Iwasita, T.; Xia, X. *J. Electroanal. Chem.* **1996**, *411*, 95.
(54) Frelink, T.; Visscher, W.; van Veen, J. A. R. *Electrochim. Acta* **1995**, *40*, 545.
(55) Sumino, M. P.; Shibata, S. *Electrochim. Acta* **1992**, *37*, 2629.
(56) Morimoto, Y.; Yeager, E. G. *J. Electroanal. Chem.* **1998**, *441*, 77.
(57) Gamboa-Aldeco, M. E.; Herrero, E.; Zelenay, P. S.; Wieckowski, A. *J. Electroanal. Chem.* **1993**, *348*, 451.
(58) Bo, A.; Sanicharane, S.; Sompalli, B.; Fan, Q.; Gurau, B.; Liu, R.; Smotkin, E. *J. Phys. Chem. B* **2000**, *104*, 7377.
(59) Koper, M. T. M. *J. Electroanal. Chem.* **1996**, *409*, 175.
(60) De Levie, R. *J. Electroanal. Chem.* **1970**, *25*, 257.
(61) Melnick, R. E.; Palmore, G. T. R. Unpublished results.
(62) Herrero, E.; Chrzanowski, W.; Wieckowski, A. *J. Phys. Chem.* **1995**, *99*, 10423.
(63) Jarvi, T. D.; Sriramulu, S.; Stuve, E. M. *J. Phys. Chem. B* **1997**, *101*, 3649.
(64) Sriramulu, S.; Jarvi, T. D.; Stuve, E. M. *Electrochim. Acta* **1998**, *44*, 1127.
(65) Vielstich, W.; Xia, X. H. *J. Phys. Chem.* **1995**, *99*, 10421.
(66) Korzeniewski, C.; Childers, C. *J. Phys. Chem. B* **1998**, *102*, 489.
(67) Childers, C.; Huang, H.; Korzeniewski, C. *Langmuir* **1999**, *15*, 786.
(68) Melnick, R. E.; Palmore, G. T. R. Submitted.
(69) Armstrong, R. D.; Henderson, M. *J. Electroanal. Chem.* **1972**, *39*, 81.
(70) Sadkowski, A. *J. Electroanal. Chem.* **1999**, *465*, 119.